DEVELOPMENTAL DYNAMICS 244:973–987, 2015
DOI: 10.1002/DVDY.24294

RESEARCH ARTICLE

Paraxis is Required for Somite Morphogenesis and Differentiation in *Xenopus laevis*

Romel Sebastián Sánchez and Sara Serafina Sánchez*

Instituto Superior de Investigaciones Biológicas (INSIBIO), CONICET-UNT, and Instituto de Biología "Dr. Francisco D. Barbieri", Facultad de Bioquímica, Química y Farmacia, Universidad Nacional de Tucumán, Chacabuco 461, San Miguel de Tucumán (T4000ILI), Argentina

Background: **In most vertebrates, the segmentation of the paraxial mesoderm involves the formation of metameric units called somites through a mesenchymal-epithelial transition. However, this process is different in *Xenopus laevis* because it does not form an epithelial somite. *Xenopus* somitogenesis is characterized by a complex cells rearrangement that requires the coordinated regulation of cell shape, adhesion, and motility. The molecular mechanisms that control these cell behaviors underlying somite formation are little known. Although the Paraxis has been implicated in the epithelialization of somite in chick and mouse, its role in *Xenopus* somite morphogenesis has not been determined. Results: Using a morpholino and hormone-inducible construction approaches, we showed that both gain and loss of function of *paraxis* affect somite elongation, rotation and alignment, causing a severe disorganization of somitic tissue. We further found that depletion or overexpression of *paraxis* in the somite led to the downregulation or upregulation, respectively, of cell adhesion expression markers. Finally, we demonstrated that *paraxis* is necessary for the proper expression of myotomal and sclerotomal differentiation markers. Conclusions: Our results demonstrate that *paraxis* regulates the cell rearrangements that take place during the somitogenesis of *Xenopus* by regulating cell adhesion. Furthermore, *paraxis* is also required for somite differentiation. *Developmental Dynamics 244:973–987, 2015*.** © **2015 Wiley Periodicals, Inc.**

Key words: *paraxis*; *tcf15*; *Xenopus*; somite; somitogenesis; cell adhesion; sclerotome; myotome; differentiation

Submitted 9 September 2014; First Decision 1 May 2015; Accepted 2 May 2015; Published online 22 May 2015

Introduction

Metamerism is an inherent feature of bodyplan in most animals. This pattern, which consists of a repeated sequence of segments along the trunk, is the prerequisite for body locomotion. In vertebrates, segmentation involves the partitioning of the presomitic mesoderm (PSM) into numerous metameric units called somites. This process passes like wave through the PSM, producing somites one by one in an anterior-to-posterior progression. Once somites are formed, they mature and differentiate into myotomal, sclerotomal and dermatomal tissue, which eventually give rise to striated muscles in the body, to the axial skeleton and to the dermis of the back, respectively (Keynes and Stern, 1988; Christ and Ordahl, 1995; Brand-Saberi et al., 1996). Somitogenesis has been highly conserved during evolution and although the behavior of the cells that drive this process differs among different vertebrate groups, morphological formation of the somite principally involves a mesenchymal-to-epithelial transition (MET) of the PSM (Ostrovsky et al., 1988; Henry et al., 2000; Kulesa and Fraser, 2002).

Grant sponsor: Consejo Nacional de Investigaciones Científicas y Técnicas (CONICET); Grant sponsor: Agencia Nacional de Promoción Científica y Tecnológica (FONCYT); Grant sponsor: Consejo de Investigaciones de la Universidad Nacional de Tucumán (CIUNT).
*Correspondence to: Sara Serafina Sanchez, CONICET, INSIBIO-CONICET-UNT. Chacabuco 461, San Miguel de Tucumán (T4000ILI), Argentina.
E-mail: ssanchez@fbqf.unt.edu.a

In contrast, somitogenesis in anurans is different from that in most vertebrates because it does not form epithelial somites (Youn and Malacinski, 1981a; Keller, 2000). In the anuran *Xenopus laevis*, somite formation is characterized by an orchestrated rotation of blocks of cells, a process that depends only on a series of cell rearrangements (Hamilton, 1969; Youn and Malacinski, 1981b). Recent studies based on confocal imaging approach showed that somite morphogenesis in this anuran begins with the mediolateral elongation of the blocks of presomitic cells which then bend anteriorly to effect a 90° turn that brings the alignment of myotome fibers parallel to the notochord (Afonin et al., 2006). During somite rotation, the distal pole of each presomitic cell exhibits filopodial extensions while the flattened medial pole moves anteriorly along the notochord. Although these studies have provided a clear understanding of the cell behavior that drives somite formation, the genetic regulation of this process is little known.

Paraxis has been described as a critical factor during vertebrate somitogenesis. This gene, a member of the basic helix–loop–helix (bHLH) -type family of transcription factors, is expressed in the anterior PSM, in the entire nascent somite, and is subsequently restricted to the dermomyotomal compartment (Quertermous et al., 1994; Burgess et al., 1995; Barnes et al., 1997; Shanmugalingam

Article is online at: http://onlinelibrary.wiley.com/doi/10.1002/dvdy.24294/abstract

and Wilson, 1998; Carpio et al., 2004; Tseng and Jamrich, 2004). Studies in mouse and chick embryos have shown that *paraxis* depletion causes failures in the epithelialization of somites leading to an improperly segmentation pattern and a loss of the anteroposterior polarity of somites (Burgess et al., 1996; Barnes et al., 1997; Johnson et al., 2001; Rowton et al., 2013). Thus, these works provided strong evidence that the function of *paraxis* is to regulate the formation of the epithelial somite during MET. In view of the differences observed in anuran somitogenesis, it is our aim to investigate the role of *paraxis* in *Xenopus* embryos.

In this work, we showed that *paraxis* is necessary for proper somite morphogenesis in *Xenopus* embryos. The alteration of *paraxis* expression affects elongation, emission of filopodia and rotation of PSM cells, causing a dramatic disorganization of somitic tissue. These results indicate that *paraxis* regulates cell behavior during somite formation. Using a series of gain and loss of function experiments, we demonstrated that *paraxis* promotes the transcription of a set of cell adhesion molecules that would be necessary to coordinate cell movements. Moreover, experiments indicate that *paraxis* is also required for the myotomal and sclerotomal differentiation of somites. Thus, our findings highlight the importance of the *paraxis* gene in the somitogenesis of *Xenopus laevis* and provide insights into the molecular bases of the regulation of this process.

Results

Gain and Loss of Function of *paraxis* Disrupts Formation of Somites

The *paraxis* gene is expressed in *Xenopus* presomitic mesoderm and persists in somite after its formation. To determine the role of *paraxis* in the somitogenesis of *Xenopus laevis*, we performed a series of loss of function experiments of *paraxis* through two different approaches. We constructed a dominant negative protein inducible with dexamethasone consisting of the N-terminal and bHLH domain of *paraxis* fused to the ligand-biding domain of the glucocorticoid receptor (*DNparaxis-GR*). This fusion protein allowed us to inhibit *paraxis* at the end of gastrulation so as not to affect such process. We also designed an antisense morpholino oligonucleotide (MO) directed against the start codon of *paraxis* (*paraxisMO*). The efficiency of the designed MO, tested by in vivo experiments, showed that *paraxisMO* inhibited translation of a green fluorescent protein (GFP) -tagged form of Paraxis (*paraxis-GFP)* in a dose-dependent manner (Fig. 1A,B,E, lane 1–3; and 1F). Besides, we prepared a Paraxis-GPF fusion construct carrying mutations in the MO recognition site (*Rparaxis-GFP*). The expression of this construct was not affected when it was coinjected with *paraxisMO* at the same doses (Fig. 1C–E, lane 5–6; and 1F), thus demonstrating the specificity of MO.

To determine the requirement for *paraxis* in somitogenesis, unilateral injections of *DNparaxis-GR* and *paraxisMO* were targeted to the PSM. Gross morphology of injected embryos was normal through gastrulation and early neurulation stages. However, from somitogenesis onward, the embryos showed a slight delay in development and a curvature along the anterior–posterior axis with the concave side corresponding to the injected half, suggesting a shortening of the axis (Fig. 2A, 36.98% n = 73; and 2C, 73.07% n = 78). In contrast, control embryos cultured in the absence of dexamethasone or injected with *CtrMO* did not develop a curved axis (Fig. 2B, n = 40; and 2D, n = 37). Additionally, we performed gain of function experiments through the microinjection of a dexamethasone inducible *paraxis* construction (*paraxis-GR*). As in the case of loss of function, we observed that *paraxis* overexpression led to a curvature of the anterior–posterior axis not detected in the control embryos (Fig. 2E, 74.46% n = 47; and 2F, n = 24); however, unlike the loss of function of *paraxis*, the concavity was opposite to the injected side, suggesting a lengthening of the axis.

A likely explanation underlying the curvature of the anterior–posterior axis could be that both gain and loss of function of *paraxis* disrupts PSM segmentation and/or somite morphogenesis. To test this hypothesis, the patterning and morphology of somites were evaluated by scanning electron microscopy (SEM). Observation of the dorsal region of the embryos injected with *DNparaxis-GR* (n = 11) revealed disorganization of the somitic tissue (Fig. 3A–C). The somites in the treated half showed a less defined shape than those of the control side. The PSM was always segmented, although sometimes a reduction in somite number was observed. Besides, analysis of the transition zone evidenced that *paraxis* knockdown led to delay in somite rotation in comparison to the control half (Fig. 3D–F), indicating that cell migration was abnormal. On the other hand, loss of function of *paraxis* by *paraxisMO* morpholino led to more severe phenotypes in comparison to the *DNparaxis-GR* injection, possibly due to its higher inhibitory ability. Paraxis morphant side displayed a drastic disorganization in somitic tissue (Fig. 3G,H, n = 12) not observed in the control side or in embryos injected with *CtrMO* (Fig. 3I,M, n = 9). Blocks of somitic cells were discernible, but their cells appeared less compact and less cohesive with each other. Furthermore, the injected cells are more rounded and filopodial protrusions are less frequent than in the control half (Fig. 3J,K), the latter being the possible cause of delayed rotation. In gain of function experiments, the SEM analyses showed that *paraxis* overexpression also produces a great disorganization in the somitic tissue, with irregular and poorly defined intersomitic boundaries (Fig. 4A, n = 11). However, unlike the *paraxis* knockdown, the *paraxis* overexpression leads to more elongated somites that causes the curvature of anterior–posterior axis. Furthermore, the observations at higher magnification did not show significant changes in the emission of filopodial extensions as were evidenced in the loss of function experiments (Fig. 4B,C).

In *Xenopus* somitogenesis, somitic cells are stacked in blocks and undergo rotation to the anterior–posterior axis of the embryos to form myotome fibers aligned parallel to the notochord. During this rotation, the morphology of nuclei progressively changes from a round to an oval/elongated shape which is correlated with the elongation of cells (Hidalgo et al., 2009). Thus, sections of normal somites display a pattern with oval nuclei forming regularly spaced stripes. To investigate whether the alteration of *paraxis* expression affects the nuclear organization and elongation of myotomal cells, we injected embryos with *paraxis-GR* mRNA or *paraxisMO* morpholino. In DAPI (4′,6-diamidino-2-phenylindole) staining sections, we observed that gain of function of *paraxis* caused a dramatic disorganization of the typical nuclear arrays (Fig. 5A,B, n = 13). The nuclei were not arranged in ordered stripes as in the control side, but rather were randomly distributed. Moreover, nuclei adopted a round shape instead of the typical elongated shaped (Fig. 5C), suggesting that cells failed to elongate and to align parallel to the notochord. Similar results were obtained following injection of *paraxisMO*

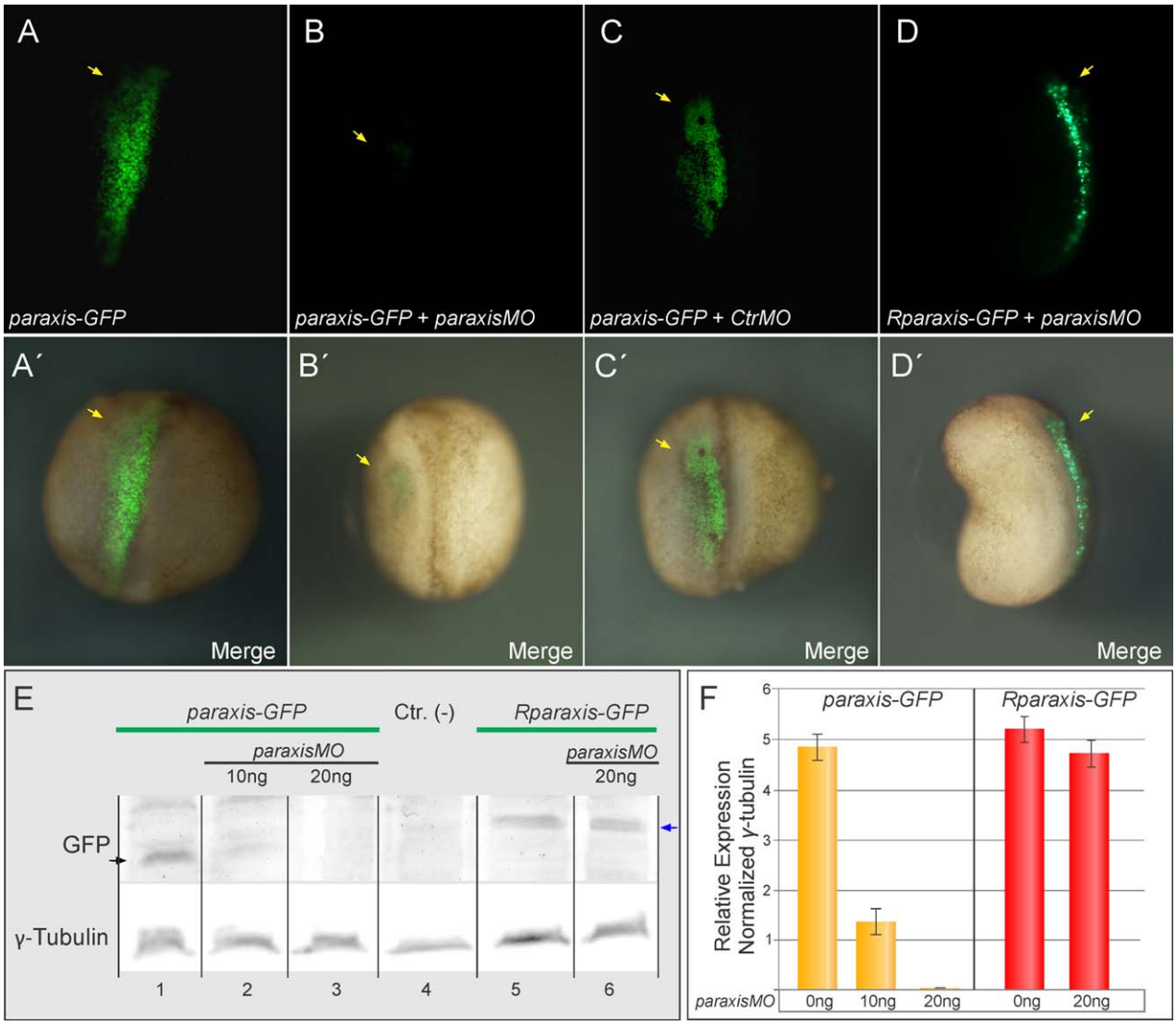

Fig. 1. Efficiency of *paraxis* antisense morpholino oligonucleotide. A–D: Dorsal views of *Xenopus laevis* embryos under a fluorescence stereoscopic microscope; anterior side is uppermost. Yellow arrows indicate the injected side. **A:** Embryos injected with mRNA that encoding *paraxis–GFP* (0.4 ng/embryo) showing GFP fluorescence. **B:** Embryos co-injected with *paraxis–GFP* mRNA (0.4 ng/embryo) and *paraxisMO* (30 ng/embryo). *paraxisMO* inhibits *in vivo* expression of *paraxis-GFP*. **C:** Embryos coinjected with *paraxis–GFP* mRNA (0.4 ng/embryo) and *CtrMO* (30 ng/embryo). **D:** Embryos coinjected with mRNA that encoding R*paraxis–GFP* (0.4 ng/embryo) and *paraxisMO* (30 ng/embryo) showing GFP fluorescence. The expression of *Rparaxis-GFP* was not affected by the presence of *paraxisMO*. **A′–D′:** Fluorescence and clear field images of each embryo are superposed and shown in merged images. **E:** Western blot assay, *paraxisMO* inhibits translation of *paraxis-GFP* in a dose-dependent manner (lane 1–3) while the expression of *Rparaxis-GFP* was not affected. Black and blue arrow indicate Paraxis-GFP and Resparaxis-GFP protein product, respectively. γ-Tubulin was used as loading control. The negative control was performed using uninjected embryos. **F**: Densitometric analysis of the expression of GFP show in E. Ctr.(-), negative control.

morpholino. In parasagittal sections, we noticed that loss of function of *paraxis* led to a severe disorganization of myotomal nuclei (Fig. 5D, n = 16) that was not observed either in the control side or in embryos injected with *CtrMO* (Fig. 5E,F, n = 8).

Taken together, the above results indicate that *paraxis* is essential for somite morphogenesis.

Paraxis Regulates Cell Adhesion During *Xenopus* Somitogenesis

The alterations observed in *paraxis* overexpression and knockdown experiments suggested that this transcription factor could be involved in the regulation of cell adhesion of the paraxial mesoderm during *Xenopus* somitogenesis. To investigate this hypothesis, mesodermal tissue explants from embryos injected with morpholino *paraxisMO* or *CtrMO* were cultured in agarose in 0.75x NAM. After a time, we observed that mesodermal explants lacking *paraxis* function began to disaggregate (Fig. 6A,B) while control explants remained intact (Fig. 6C). Cell disaggregation was greater as the concentration of *paraxisMO* increased, indicating that loss of function of *paraxis* led to a decreased cell adhesion in a dose-dependent manner.

This decrease in cell adhesion could be due to the loss of expression of adhesion molecules. To examine the effect of embryo-derived *paraxis* depletion on gene expression, particularly with respect to adhesion molecules, mesodermal explants

Fig. 2. Gross morphology of embryos in experiments of loss and gain function of *paraxis* gene. Embryos were unilaterally injected with 0.5 ng of *DNparaxis-GR* mRNA (**A**), 25 ng of *paraxisMO* (**C**), 25 ng of *CtrMO* (**D**), or 1 ng of *paraxis-GR* mRNA (**E**). **B,F:** Uninjected control embryos. The alteration of the expression of *paraxis* in the paraxial mesoderm leads to curvature of anteroposterior axis of the embryos.

from the experiment described above were analyzed by semi-quantitative reverse transcriptase-polymerase chain reaction (RT-PCR) at the neurula stage. We found that expression of the predominant cadherins *E-cadherin* and *EP-cadherin*, the tight junction associated protein *occludin*, and the fibronectin receptor *integrin 5α* were significantly downregulated in a dose-dependent manner by *paraxis* knockdown (Fig. 6D,E). Similarly, we observed that the expression of the transcription factor *FoxC1*, an important regulator of cell adhesion in the mesodermal layer (Cha et al., 2007), was also severely downregulated in a dose-dependent manner by *paraxis* depletion (Fig. 6D,E). This last finding was confirmed by whole-mount in situ hybridization in which *paraxis* knockdown led to reduction of *FoxC1* gene expression (Fig. 7). Furthermore, we analyzed the expression of extracellular matrix protein fibronectin. In this experiment, the embryos were bilaterally injected with *paraxisMO* or *CtrMO* and evaluated by Western blot assay in the tail-bud stage. We found that *paraxis* depletion led to a mild decrease of fibronectin expression indicating that the extracellular matrix is also affected (Fig. 8).

Thus, the loss of function of *paraxis* caused a reduction in the expression of genes associated with cell/cell and cell/matrix interaction, which would explain the loss of cell adhesion, indicating that *paraxis* is necessary for the regulation of expression of cell adhesion molecules in *Xenopus* somitogenesis.

We then examined whether the gain of function of *paraxis* affected the expression of genes associated with cell adhesion. To test this point, mesodermalized animal caps from embryos injected with *paraxis-GR* mRNA were cultured in the presence or absence of dexamethasone until the neurula stage and processed for RT-PCR. In these experiments, we found that *paraxis* overexpression upregulated the expression of the transcription factor *FoxC1* and of the adhesion molecules *E-cadherin* and *occludin* while *EP-cadherin* was not significantly affected (Fig. 9), thereby confirming the key role of *paraxis* in the regulation of cell adhesion during somitogenesis.

Paraxis is Required for Somite Differentiation

We next determined whether alteration of *paraxis* expression affected somite differentiation in *Xenopus laevis*. Previous studies in mouse showed that this gene is necessary for hypaxial myogenesis and dermomyotome formation (Wilson-Rawls et al., 1999). To establish the role of *paraxis* in *Xenopus* somite myogenesis, the embryos were unilaterally injected with *DNparaxis-GR* mRNA or with *paraxisMO* morpholino and analyzed by *in situ* hybridization. In these experiments, we found that loss of function of *paraxis* provoked a drastic reduction in the expression of *MyoD* and *Myf-5* myogenic markers (Fig. 10A–C,E–G, I–K,P). In contrast, control embryos did not show significant changes in the expression of these markers (Fig. 10D,H,M). The specificity of *paraxisMO* was corroborated by rescue experiments by coinjecting *paraxisMO* with *Rparaxis-GFP* mRNA construction (Fig. 10N–P), which resulted in the restitution of *MyoD* and *Myf-5* expression. Additionally, we evaluated the expression of myotome terminal differentiation marker 12/101, finding that *paraxis* depletion leads to a loss of expression of this gene (Fig. 10Q–T). These results were confirmed in mesoderm explant experiments, in which *paraxis* knockdown led to a dose-dependent reduction of *MyoD*, *Myf-5* and *pax3* expression (Fig. 11), indicating that *paraxis* is required for normal myogenic differentiation of somites.

To determine whether *paraxis* promotes muscle differentiation, we overexpressed *paraxis* in *Xenopus* embryos and analyzed the expression of myogenic markers by *in situ* hybridization. We found that injection of *paraxis-GR* mRNA led to an increase in *Myf-5* and *MyoD* expression (Fig. 12A–C,E–F,H) that was not observed in control embryos (Fig. 12D,G). These results were confirmed in animal cap assays where *paraxis* induced ectopic expression of *MyoD*, *Myf-5*, and *pax3* genes (Fig. 13), thus evidencing that the *paraxis* gene plays an active role in the regulation of myogenic differentiation of somites in *Xenopus laevis*.

We also analyzed the role of *paraxis* in sclerotomal differentiation of somites. Loss of function approaches using *paraxisMO* showed that *paraxis* depletion produced a reduction in *pax1* and *pax9* sclerotomal markers and *col2a* chondrogenic marker (Fig. 14). Likewise, *paraxis* knockdown in mesoderm explants experiments led to the downregulation of *pax1*, *pax9*, and *uncx* expression (Fig. 15), suggesting that *paraxis* is required for sclerotomal lineage differentiation of somites. Moreover, ectopic *paraxis* overexpression in animal cap assays was unable to induce the expression of *pax1*, *pax9*, and *uncx* genes (data not shown), indicating that *paraxis* by itself is not sufficient to induce sclerotomal differentiation of somites.

Discussion

Our analysis of the *paraxis* function in *Xenopus* somitogenesis revealed that its expression is required for proper somite

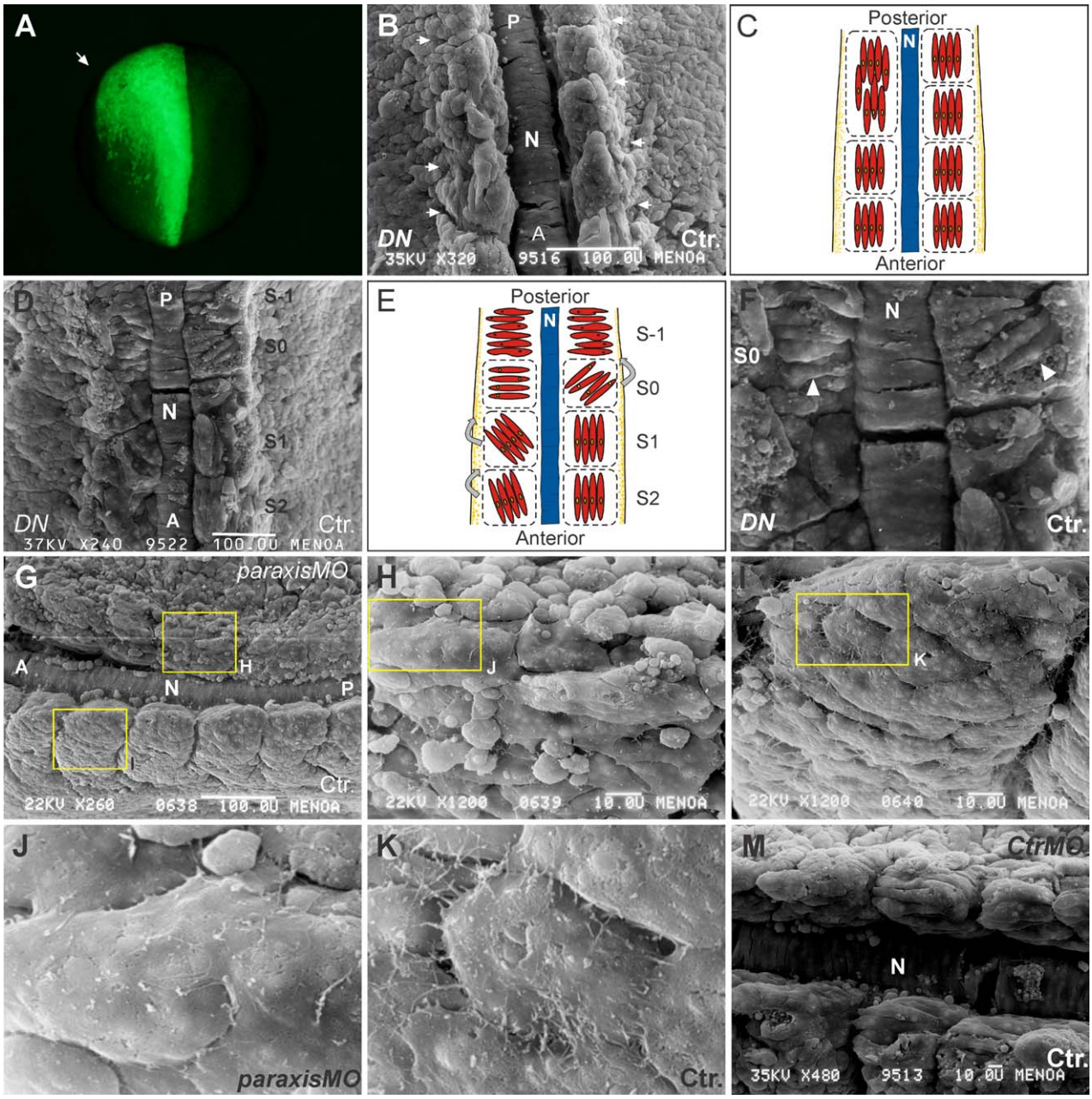

Fig. 3. SEM analysis of *Xenopus* somitogenesis in *paraxis* knockdown experiments. Dorsal views of *Xenopus* embryos at the tail-bud stage. Embryos were unilaterally injected with 1 ng of *DNparaxis-GR* mRNA (B,D,F), 40 ng of *paraxisMO* (G–K) or 40 ng of *CtrMO* (M) together with the lineage tracer FDA. **A:** The injected side of the embryos was determined by observing the fluorescence of FDA. **B:** Knockdown of *paraxis* using *DNparaxis-GR* leads to the formation of irregular intersomitic boundaries and sometimes fusion of somites was observed. White arrows indicate intersomitic boundaries. **C:** Schematic representation of B. **D:** Knockdown of *paraxis* causes a delay in the rotation of somitic cells during somitogenesis. **E:** Schematic representation of D. **F:** Enlargement of D at the level of the transition zone (S0). White arrowheads indicate the orientation of presomitic cells. **G:** Loss of function of *paraxis* using *paraxisMO* morpholino leads to severe cellular disorganization. **H,I:** Micrographs of the somite injected with *paraxis-MO* and of uninjected control side, respectively, in which is observed the dermatome cells. **J,K:** Enlargement of H and I, respectively, in which filopodial extensions are shown. **M:** Uninjected control embryos. A, anterior; N, notochord; P, posterior; S, somite numbers, according to the nomenclature of somitogenesis (Pourquie and Tam, 2001).

morphogenesis. Here we propose that the *paraxis* gene regulates somitogenesis, at least partly, by modulating the expression of a set of cell adhesion molecules necessary for the transmission of traction force throughout the somitic unit and of information necessary to coordinate those cell movements. In addition, we found that *paraxis* is required for myotomal and sclerotomal differentiation of somites.

Paraxis Regulates Somite Morphogenesis in *Xenopus* Through Modulation of Cell Adhesion

Perturbation of the *paraxis* function affected somite morphogenesis in *X. laevis*. These phenotypic changes were demonstrated by both gain and loss of function of *paraxis* by different experimental approaches.

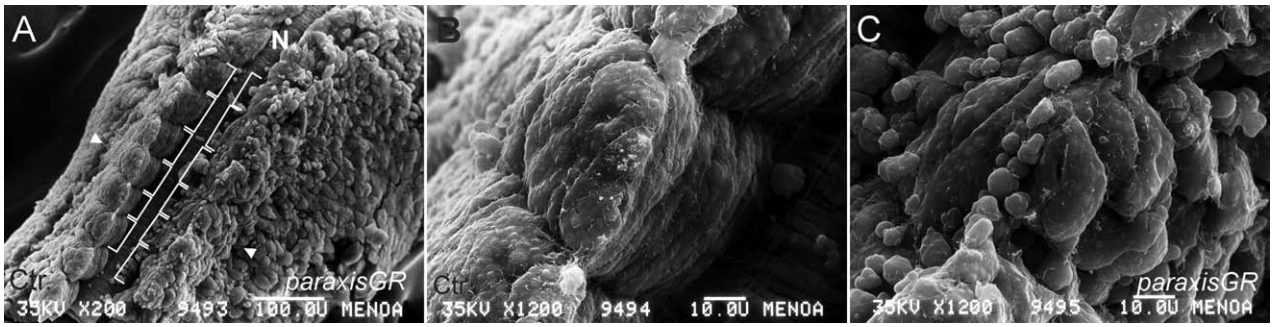

Fig. 4. SEM analysis of *Xenopus* somitogenesis in *paraxis* overexpression experiments. Dorsal views of *Xenopus* embryos at the tail-bud stage. Embryos were unilaterally injected with 1 ng of *paraxis-GR* mRNA together with the lineage tracer FDA. **A:** *paraxis* overexpression leads to the formation of irregular intersomitic boundaries and a lengthening of the somites (indicated by brackets) that was not observed in control side (indicated by brackets). **B:** Magnification of control side of A at the level of white arrowhead. **C:** Magnification of morphant side of A at the level of white arrowhead. N, notochord.

Injected embryos analyzed at the tail-bud stage showed that *paraxis* knockdown and overexpression led to a shortening and a lengthening of the anteroposterior axis, respectively. The main force that directs axis elongation is convergent extension (Keller and Danilchik, 1988); however, we dismissed the possibility of this phenotype being the result of the disruption of this process because the shortening of the axis occurred even when dexamethasone-inducible constructs were activated in the early tail-bud stage. We propose that shortening and lengthening of the anteroposterior axis is caused by an alteration of cell movements associated with somite formation.

Somitogenesis in *X. laevis* is characterized by complex cellular rearrangements in which PSM cells undergo coordinated changes in cell motility, shape, and adhesion. In this process, blocks of mediolaterally elongated presomitic cells increased the number of filopodial projections and underwent a 90° rotation around the dorsoventral axis to finally elongate and align themselves parallel to the notochord (Afonin et al., 2006). SEM and nuclear

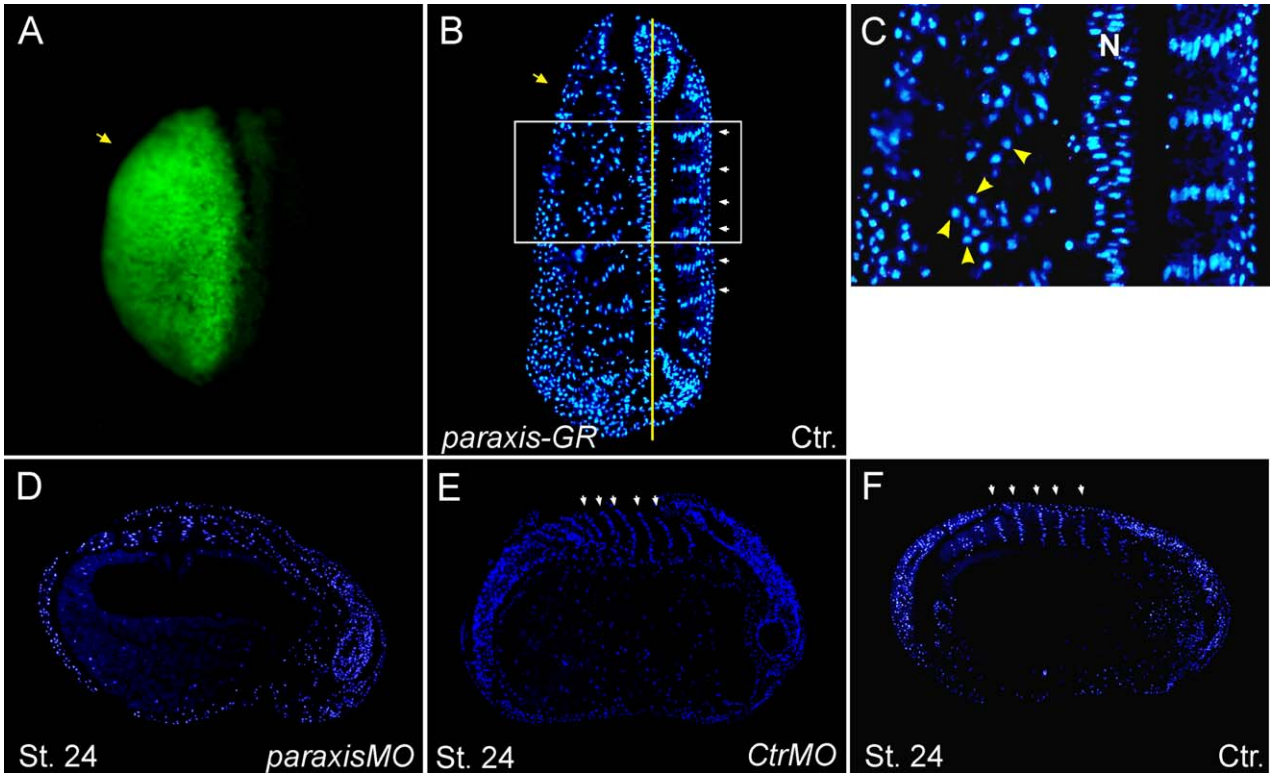

Fig. 5. Analysis of nuclear organization of myotomal cells in experiments of gain and loss of function of the *paraxis* gene. Sections were obtained from tail-bud stage embryos unilaterally injected with 1 ng of *paraxis-GR* mRNA (B,C), 40 ng of *paraxisMO* (D) or 40 ng of *CtrMO* (E) together with the lineage tracer FDA. B,C: Frontal section with anterior side uppermost; (D–F) parasagittal section with anterior side to the right. **A:** The injected side of the embryos was determined by observing the fluorescence of FDA. **B:** The overexpression of *paraxis* leads a loss of nuclear organization. Yellow arrows indicate the injected side and white arrows indicate the alignment of nuclei miotomal cells (control side). **C:** Enlargement of B at the level of white rectangle, wherein is observed the rounded shape of the cells nuclei of the treated side of the embryo (yellow arrowheads). **D:** Loss of function of *paraxis* leads to a severe disorganization of myotomal nuclei. **E:** The microinjection of *CtrMO* does not affect nuclear organization. **F:** Uninjected control embryos. N, notochord.

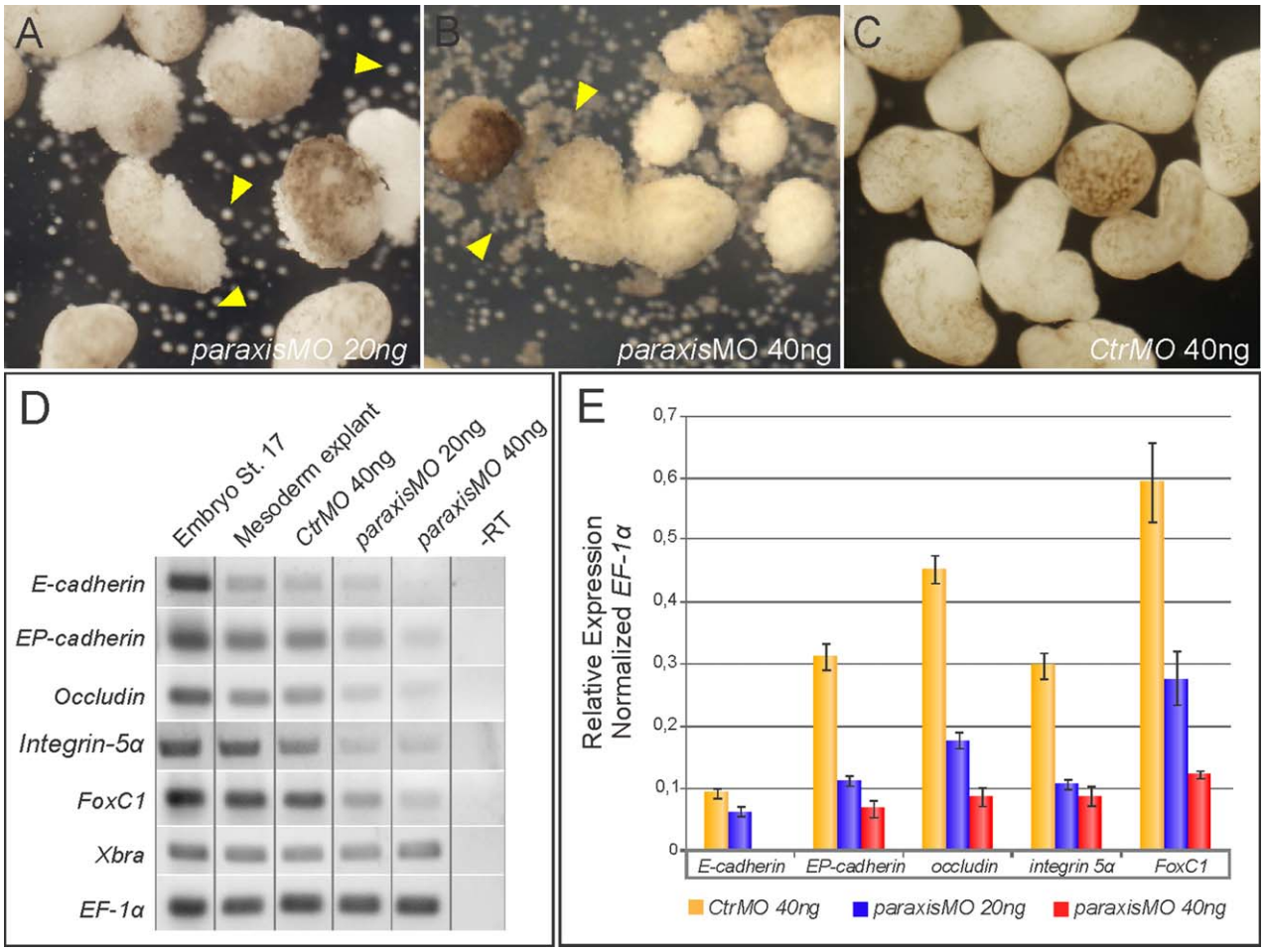

Fig. 6. Cell adhesion assay in mesoderm explants. The explants were obtained from gastrula embryos bilaterally injected with 20 ng of *paraxisMO* (A), 40 ng of *paraxisMO* (B) or 40 ng of *CtrMO* (C) and cultured until stage 17. **A,B:** knockdown of *paraxis* gene leads to disaggregation cell of the mesoderm explants tissue. Yellow arrows indicate disaggregating cells. **C:** Control mesoderm explants. **D:** RT-PCR semiquantitative analysis in mesoderm explants. Whole embryos and mesoderm explants from uninjected embryos were used as positive control and explants control, respectively. Knockdown *paraxis* causes a dose-dependent decrease in the expression of adhesion molecules. **E:** Densitometric analysis of the expression of adhesion molecules show in D. –RT, negative control.

staining analysis showed that *paraxis* knockdown caused a great disorganization of the somitic tissue. The paraxial mesoderm was segmented although the intersomitic boundaries were irregular and sometimes difficult to discern. Myotomal cells did not achieve correct elongation and the nuclei failed to align themselves perpendicularly to the notochord. A close examination of these cells revealed a loss of filopodial protrusions and a delay in their rotation, indicating that they no longer migrated normally. Thus, we propose that *paraxis* is required for correct rotation and elongation of presomitic cells in *Xenopus* somitogenesis. These results allow us to conclude that although cell behavior involved in somites formation in *Xenopus* is very different from those observed in other vertebrates, the role of Paraxis is conserved, its central function being the regulation of somite morphogenesis.

In addition, *paraxis* knockdown experiments demonstrated that somitic cells are less compact and less cohesive between each other, suggesting an alteration in cell–cell adhesion. To investigate this hypothesis, we performed in vitro experiments and found that loss of function of *paraxis* led to cellular disaggregation of mesodermal tissue explants. Therefore, these results indicate that *paraxis* regulates the adhesive properties of the presomitic mesoderm during somite formation. Analysis of cell turning behavior during *Xenopus* somitogenesis revealed that cells comprising the block of prospective somites do not move "*en bloc*" but instead move individually in a coordinated manner

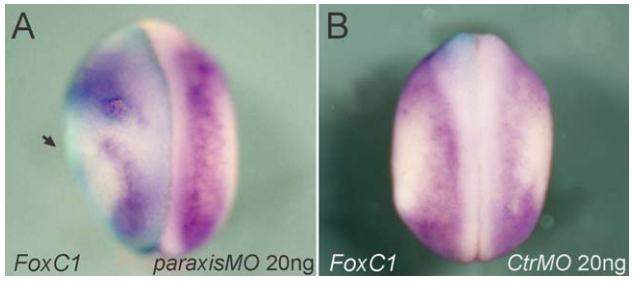

Fig. 7. *paraxis* knockout disrupts the expression of the cell adhesion marker *FoxC1*. Embryos were unilaterally injected with 20 ng of *paraxisMO* or 20 ng of *CtrMO*, cultured until neurula stage and subsequently processed for *in situ* hybridization assay. **A:** The loss of function of *paraxis* reduces the expression of the *FoxC1* gene in PSM (indicated by arrow). **B:** Control embryo injected with *CtrMO*.

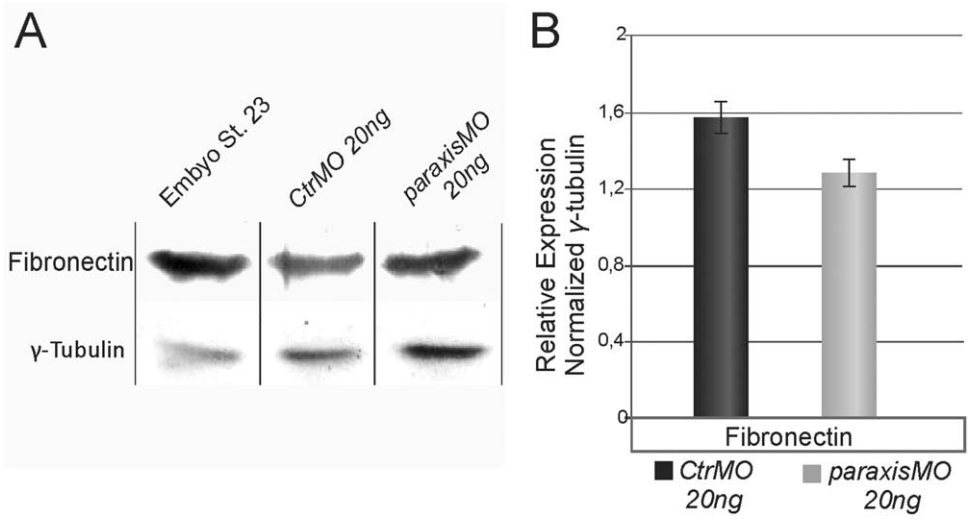

Fig. 8. *paraxis* knockout reduces the Fibronectin expression. Embryos were bilaterally injected with 20 ng of *paraxisMO* or 20 ng of *CtrMO*, cultured until tail-bud stage and subsequently processed for western blot assay. **A:** The loss of function of *paraxis* leads to a mild reduction of Fibronectin expression. γ-Tubulin was used as loading control. **B:** Densitometric analysis of the expression of Fibronectin shown in A.

(Wilson et al., 1989; Keller, 2000; Afonin et al., 2006). Youn and Malacinski (1981b) observed that cells adjacent to the notochord are the first to change orientation. They proposed that these cells would be responsible for initiating the rotation of somites, inducing other cells to rotate. In their model, cell–cell interactions play a pivotal role in the coordination of movement as later demonstrated by Giacomello et al. (2002). In agreement with the above results, we propose that the lack of cell–cell and cell–EMC interaction, caused by loss of function of *paraxis* may have affected the sensing mechanisms required to coordinate movements during the rotation of somites. Cells maintain their migratory capability but they lose the ability to crawl across each other, resulting in the random movement of myotomal cells causing the disorganization of somitic tissue.

The disruption in cell adhesion triggered by *paraxis* knockdown was confirmed by semiquantitative RT-PCR. We found that *paraxis* is necessary for the expression of the molecules associated with cell–cell adhesion *E-cadherin*, *EP-cadherin*, and *occludin*. Consistent with our results, previous studies showed that *E-cadherin* and *EP-cadherin* depletion affected the coordination of cell movements during *Xenopus* somite formation, generating a phenotype similar to those obtained in *paraxis* knockdown experiments (Giacomello et al., 2002). Additionally, we evidenced a reduction in the expression of the *FoxC1* gene. This gene encodes a transcription factor which modulates cell–cell adhesion of paraxial mesoderm through the regulation of the expression of *EP-* and *E-cadherin* as well as of the members of the Ephrin/EphR signaling families (Cha et al., 2007).

Moreover, we also found that *paraxis* is required for cell–ECM interaction. Loss of function of *paraxis* causes a reduction in the expression of fibronectin and *integrin α5* fibronectin receptor. In agreement with this result, *integrin α5* has been shown to be

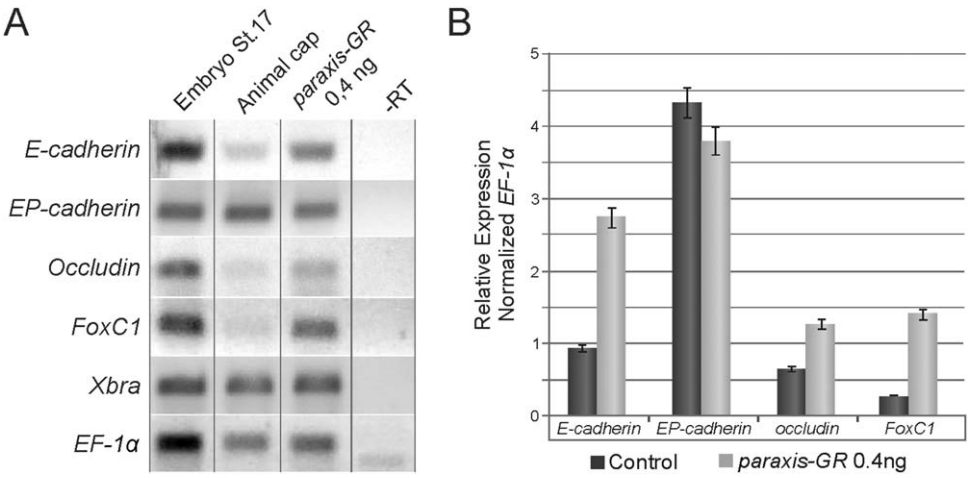

Fig. 9. Overexpression of *paraxis* increases cell adhesion. **A:** RT-PCR semiquantitative analysis of adhesion markers in animal cap explants obtained from embryos injected with 0.4 ng of *paraxis-GR* mRNA and cultured in the presence of Activin A and dexamethasone until stage 17. Injected explants cultured in the absence of dexamethasone were used as caps control, the positive control consisting of whole embryos at stage 17. The gain of function of *paraxis* causes an increase in the expression of molecules involved in cell adhesion. **B:** Densitometric analysis of the expression of adhesion molecules show in A. –RT, negative control.

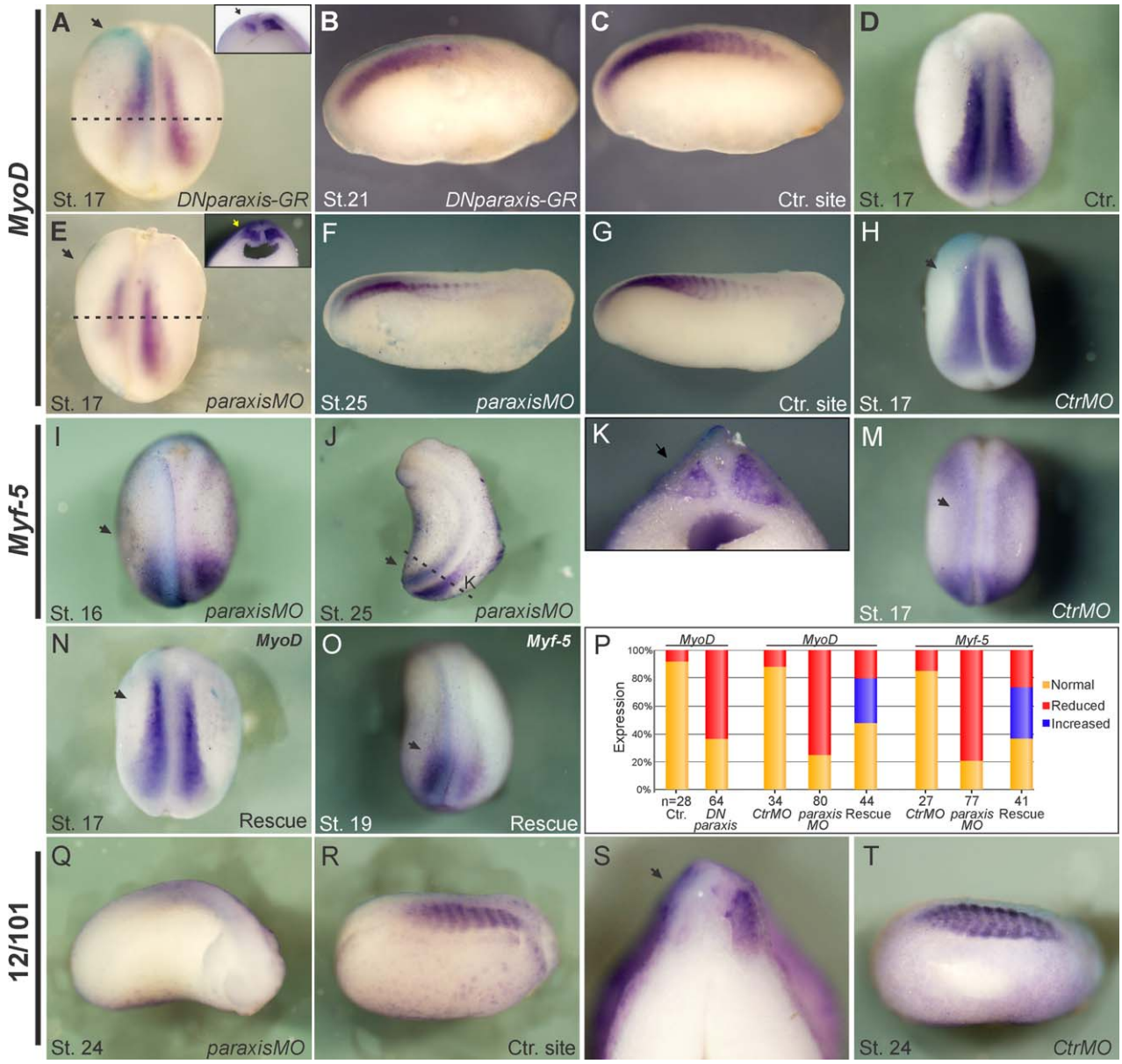

Fig. 10. *paraxis* depletion disrupts the expression of myogenic markers. Embryos were unilaterally injected with 1 ng of *DNparaxis-GR* mRNA (A–D), 40 ng of *paraxisMO* (E–G, I–K, and Q–S), 40 ng of *CtrMO* (H, M and T), or a blend of 40 ng of *paraxisMO* and 0.2 ng of *Rparaxis-GFP* mRNA (N and O), and subsequently processed for *in situ* hybridization assay (A–O) or immunohistochemical (Q–T). **A–C,E–G:** The loss of function of *paraxis* reduces the expression of the *MyoD* myogenic marker in PSM and somites (indicated by arrow). **D:** Control embryo injected with the *DNparaxis-GR* mRNA and cultured in the absence of dexamethasone. **H:** *CtrMO* morpholino does not affect the expression of *MyoD* myogenic marker. **I,J:** The loss of function of *paraxis* reduces the expression of *Myf-5* myogenic marker. **K:** Transverse section at the dotted line of J. **M:** *CtrMO* does not affect the expression of *Myf-5*. **N,O:** The downregulation of *MyoD* and *Myf-5* expression by *paraxisMO* is rescued by coinjection with *Rparaxis-GR* construct. **P:** Numerical summary illustrating the penetrance of effect of *paraxis* knockdown and the rescue of myogenic markers expression. **Q:** The loss of function of *paraxis* reduces the expression of the 12/101 myogenic marker. **R:** Control side of Q. **S:** Transverse section of Q. **T:** Control embryo. Insets A and E, transverse section at the dotted line.

important as the cells rotate to form aligned myotome fibers (Kragtorp and Miller, 2007).

Overexpression experiments reveled that *paraxis* is capable of inducing the ectopic expression of *FoxC1*, *occludin*, and *E-cadherin* genes which indicate that Paraxis plays an active role in the regulation of cell adhesion. Our findings are supported by a recent study performed in mouse, which demonstrated that the loss of function of *paraxis* causes a deregulation in the expression of a set of genes associated with cell–cell and cell–EMC adhesion and with cytoskeletal organization (Rowton et al., 2013).

Thus, we conclude that *paraxis* regulates somite morphogenesis in *Xenopus laevis*, at least partly, through control of the expression of a set of genes associated with cell–cell and cell–EMC adhesion.

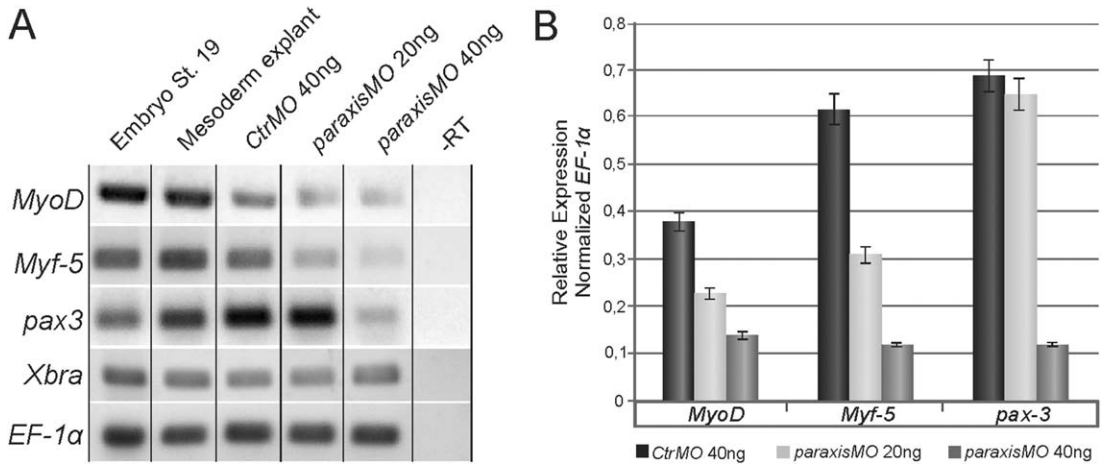

Fig. 11. Quantification of the effect of *paraxis* knockdown on myogenic expression in mesoderm explants assay. **A:** RT-PCR semiquantitative analysis of expression of myogenic markers in mesoderm explants obtained from embryos injected with 20 and 40 ng of *paraxisMO*, 40 ng of *CtrMO* or uninjected embryos. Loss of function of *paraxis* causes a dose-dependent decrease in the expression of myogenic markers. **B:** Densitometric analysis of A. –RT, negative control.

Paraxis is Required for Somite Differentiation

Studies performed in mouse showed that Paraxis is not only involved in the morphogenesis of somites but also participates in their differentiation (Burgess et al., 1996; Wilson-Rawls et al., 1999). Here we showed by loss of function experiments that *paraxis* is necessary for the normal expression of *MyoD* and *Myf-5* genes. These molecules, defined as myogenic determination factors, participate in the activation of skeletal muscle gene expression during myogenic differentiation of somites (Hopwood et al., 1989, 1991; Ludolph et al., 1994; Maves et al., 2007; Buckingham and Vincent, 2009; Hinits et al., 2009). We also found that *pax3* is downregulated by *paraxis* depletion. This result is supported by a recent work showing that *paraxis*, in cooperation with *Mef2d*, activates the expression of *Meox2* gene, which acts upstream of *pax3* expression during dermomyotome formation (Della Gaspera et al., 2012). Pax3 is a dermomyotomal marker whose expression is essential for both formation of the hypaxial myotome and migration of the myogenic progenitor cells into the limb (Franz et al., 1993; Goulding et al., 1993; Tajbakhsh et al., 1997; Tremblay et al., 1998). Furthermore, in overexpression experiments, *paraxis* was able to induce ectopic expression of *MyoD*, *Myf-5*, and *pax3*, demonstrating that it plays an active role in myogenic regulation. Thus, we propose that *paraxis* participates in a regulatory pathway that promotes the transcription of genes necessary for the myogenic differentiation of somites. This hypothesis is supported by the reduced expression of myotome terminal differentiation marker 12/101 observed in the loss of function of *paraxis* assays.

Prior studies in mouse showed that Paraxis is required for the expression of Pax1, Nkx3.1, Bapx1, and Sox9, which are crucial factors in vertebral column formation, suggesting that this gene

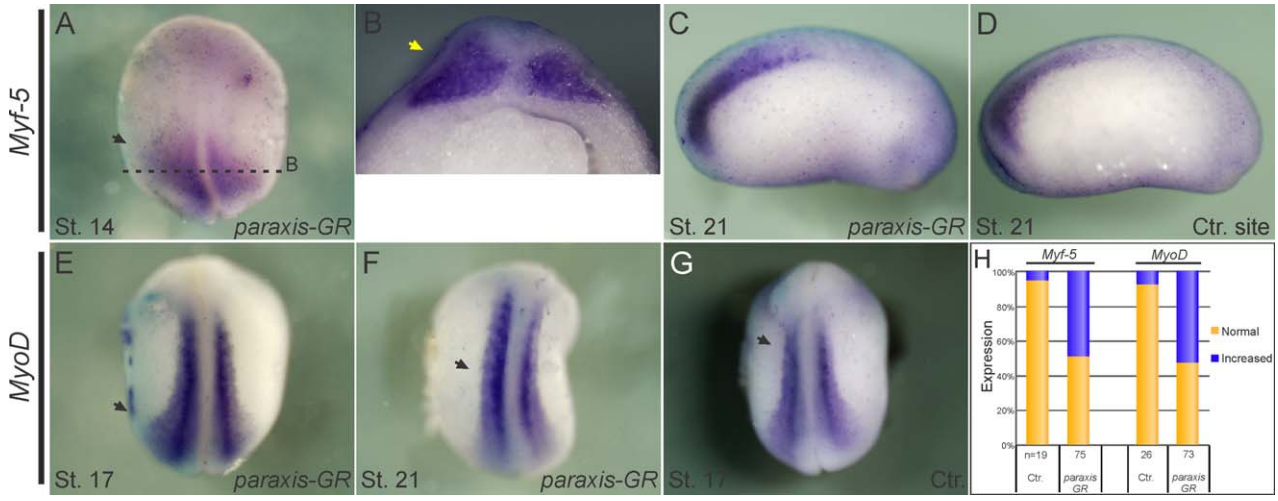

Fig. 12. Gain of function of *paraxis* increases myogenic markers expression. Embryos were unilaterally injected with 1 ng of *paraxis-GR* mRNA and processed for *in situ* hybridization assay. **A–C,E–F:** The gain of function of *paraxis* increases the expression of myogenic markers *Myf-5* and *MyoD* (indicated by arrow). **B:** Transverse section at level of the dotted line. **D:** Control side of C. **G:** Control embryo cultured in the absence of dexamethasone. **H:** Numerical summary illustrating penetrance of gain of function of *paraxis* in myogenic markers expression.

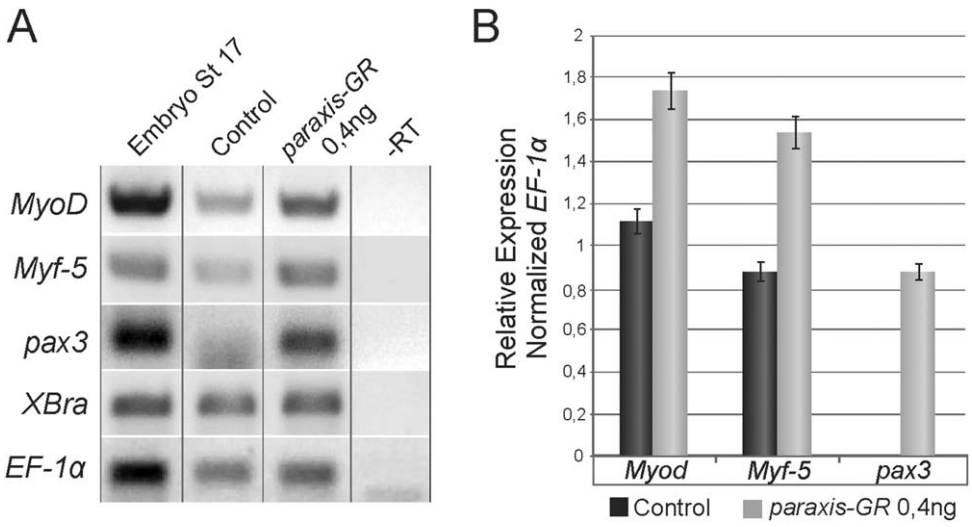

Fig. 13. Quantification of the effect of *paraxis* gain of function on myogenic markers expression in animal caps assay. **A:** RT-PCR semiquantitative analysis of myogenic markers in animal cap explants obtained from embryos injected with 0.4 ng of *paraxis-GR* mRNA and cultured in the presence of Activin A and dexamethasone. Injected explants cultured in the absence of dexamethasone were used as caps control. The gain of function of *paraxis* causes an increase in the expression of *MyoD* and *Myf-5* genes and is capable of inducing *pax3* expression in the animal caps tissue. **B:** Densitometric analysis of A. –RT, negative control.

plays a significant role in sclerotome differentiation (Wilson-Rawls et al., 2004; Takahashi et al., 2007). Similarly, we also found that *paraxis* is necessary for normal sclerotomal differentiation in *Xenopus*. Our results showed that *paraxis* knockdown caused a reduction in the expression of *pax1*, *pax9*, and *uncx* sclerotomal markers and in *Col2a* chondrogenic marker. These genes play a pivotal role in cell proliferation and chondrogenic differentiation of sclerotome during axial skeleton formation (Wallin et al., 1994; Peters et al., 1999; Leitges et al., 2000; Mansouri et al., 2000; Rodrigo et al., 2003; Sanchez and Sanchez, 2013). However, in our experiments *paraxis* alone was not able to induce ectopic expression of these sclerotomal genes, which could mean that other factors would be required for *paraxis* to promote the expression of its target genes in the sclerotome or that reduction in the expression of sclerotomal genes observed in *paraxis* knockdown experiments is only a consequence of the disruption of somite morphogenesis. Further studies are needed to determine the exact role of the *paraxis* gene in the sclerotomal differentiation of *Xenopus*.

Experimental Procedures

Embryo Manipulation

Adult male and female *Xenopus laevis* specimens were stimulated with 400 IU and 800 IU of human chorionic gonadotropin (HCG–Elea Lab), respectively. Fertilized eggs were obtained after natural single-pair mating and they were dejellied with 2% cysteine hydrochloride (pH 7.8) and cultured in 0.1x NAM. They were staged according to the Nieuwkoop and Faber tables (1967).

Antisense Morpholino Oligolucleotide Design and Synthesis

By datebase research we identified one *Xenopus paraxis* allele (Gene Bank accession N° AY599421). Antisense morpholino oligonucleotide was designed to complement the 5′ regions of this allele between −9 and +19 (*paraxisMO*: 5′TCA TGG TGA AGG CCA TGT GAG CCC T′3). As a control, we used a standard MO (*CtrMO*: 5′CCT CTT ACC TCA GTT ACA ATT TAT A′3).The morpholinos were synthesized by Gene Tool LLC.

DNA Constructs and Capped mRNA Synthesis

To test the efficacy of *paraxisMO*, a *paraxis-GFP* fusion construct was generated by high fidelity PCR using pBlueScripSK*paraxis* plasmid as the template (kindly provided by Dr. Naoto Ueno, NIBB, Okazaki, Japan) and the following primers: 5′-GGA TCC GCC CAG GGC TCA CAT G (underlined, *Bam*HI restriction site) and 5′-CTC GAG TCA TCG CAA TGT GTT AAG-3′ (underlined, *Nco*I restriction site). The fragment containing the N-region of *paraxis* was cloned into the pGEM®-Easy vector, amplified and then subcloned directionally into *Bam*HI and *Nco*I pCS2+eGFP vector. For rescue of morpholino knockdown experiments, a full-length *paraxis* fusion construct lacking 5′UTR (*Rparaxis-GFP*) was constructed in the same way as described above. This construct also carries three mismatches, keeping the amino acid sequence of wt*paraxis*. The primers used were: 5′-GGA TCC ATG GCa TTt ACa ATG ATC CG-3′ (underlined, *Bam*HI restriction site; lowercase letters indicate mismatched bases) and 5′-CCA TGG TGC CTC CAG TCT TGG CAG CGG-3′ (underlined, *Nco*I restriction site). In vitro transcribed capped mRNA of these constructs were coinjected with different amounts of *paraxisMO or paraxis-Ctr.* and GFP expression was evaluated by fluorescence stereomicroscope (OLYMPUS MVX10) and Western Blot.

For studies of *paraxis* overexpression, a dexamethasone-inducible *paraxis* construct (*paraxis-GR*) was generated. The fragment encoding the hormone-binding domain (amino acids 512-777) of the human glucocorticoid receptor (*hGR*) was added at the C-terminal end of the coding sequence of full-length *paraxis* protein. The following primers were used: 5′-GAA TTC ATG GCC TTC ACC ATG ATC CGT TCC-3′ (underlined, *Eco*RI restriction site) and 5′-GAG CTC CAT CGC AAT GTG TTA AGC CCC-3′ (underlined, *Sac*I restriction site). The coding sequence of *paraxis*

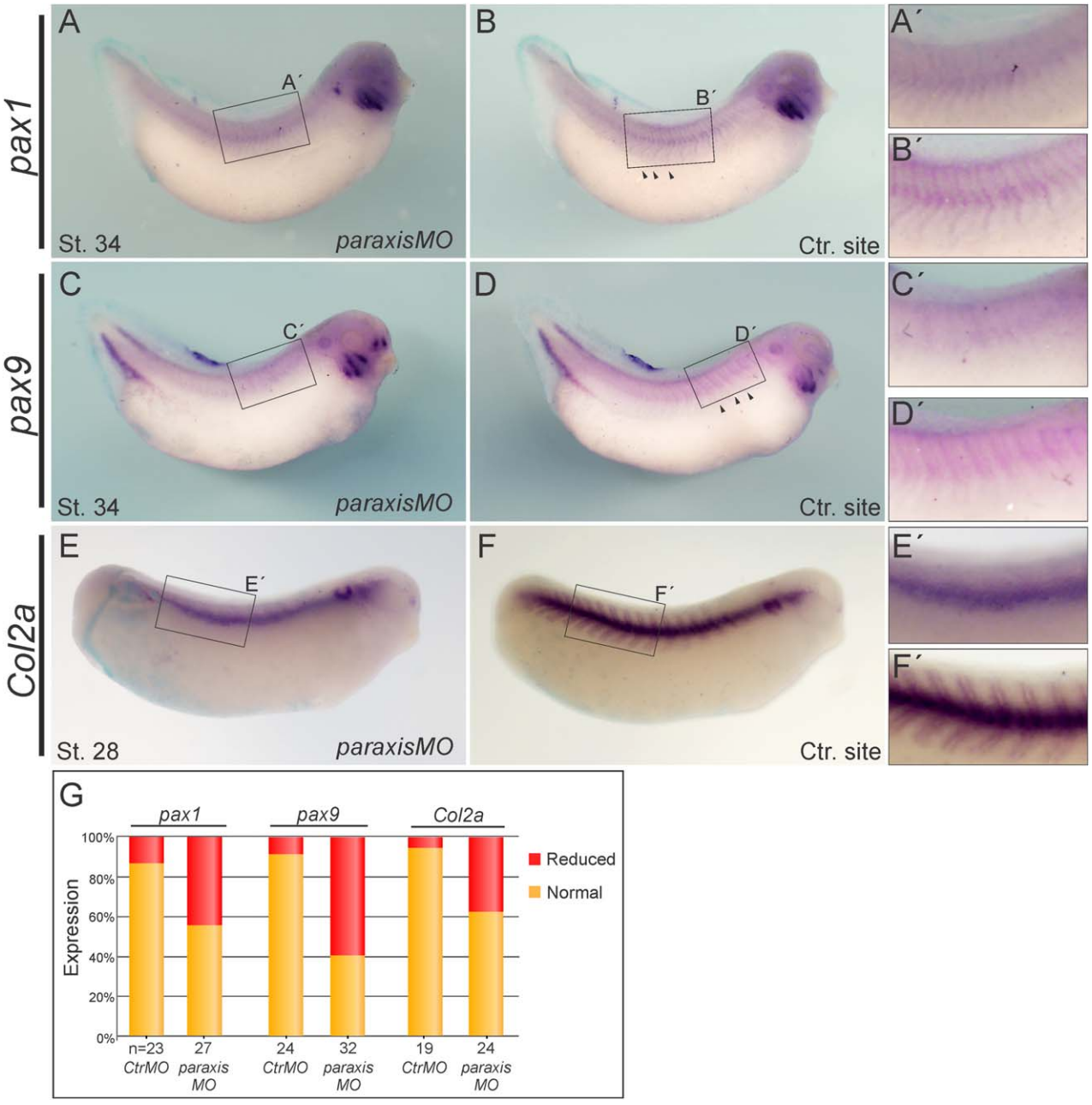

Fig. 14. *paraxis* knockdown disrupts the expression of chondrogenic markers. Embryos were unilaterally injected with 10 ng of *paraxisMO* and processed for *in situ* hybridization assay. **A,C,E:** The loss of function of *paraxis* reduces the expression of chondrogenic markers *pax1*, *pax9* and *Col2a*, respectively. **B**,**D**,**F:** Control side of embryo. **A′–F′:** Enlargement of A–F at the level of the black rectangle. **G:** Numerical summary illustrating penetrance of the loss of function of *paraxis* in chondrogenic markers expression.

was cloned into the pGEM®-Easy vector, amplified and then subcloned directionally into *EcoRI* and *SacI* in pCS2+*hGR* vector. Additionally, we constructed an inducible dominant-negative protein for *paraxis* (*DNparaxis-hGR* or *DN*). *DNparaxis-hGR* was generated by truncation of the C-terminus end of *paraxis* gene. The following primers were used: 5′-GAA TTC ATG GCC TTC ACC ATG ATC CGT TCC-3′ (underlined, *Eco*RI restriction site) and 5′-GAG CTC CAC AGC ACG TTG GCC -3′ (underlined, *Sac*I restriction site). This fragment was cloned in the pGEM®-Easy vector and directionally subcloned into pCS2+*hGR* vector. The embryos or tissue explants injected with 0.4–1 ng of *paraxis-GR* or DN*paraxis-GR* mRNA were treated at the end of the gastrulation (stage 13–15) with 10 μM of dexamethasone in NAM. All plasmids were fully sequenced.

Microinjection and Explant Assays

Xenopus embryos at the two- to four-cell stage were injected with capped mRNA or morpholino alone or together with the lineage tracer fluorescein dextran amine (FDA) in 0.1x NAM containing 3% Ficoll-400.

For animal cap assays, capped *paraxis-GR* mRNA was injected into the animal pole of both blastomeres of two-cell stage embryos. Animal caps were dissected at stage 9 and cultured in

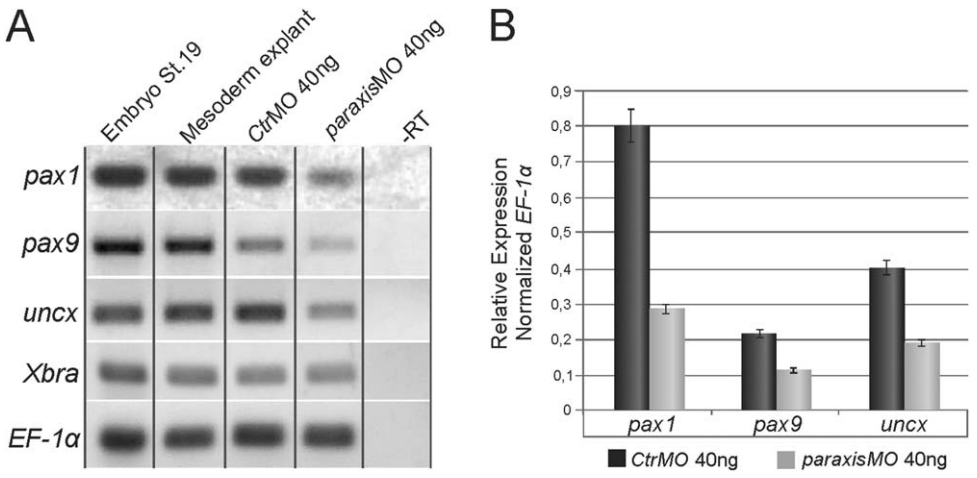

Fig. 15. Quantification of the effect of *paraxis* knockdown on chondrogenic expression in mesoderm explants assay. **A:** RT-PCR semiquantitative analysis of chondrogenic markers in mesoderm explants obtained from embryos injected with *paraxisMO*, *CtrMO* or uninjected. The loss function of *paraxis* causes a decrease in the expression of *pax1*, *pax9*, and *uncx* chondrogenic markers. **B:** Densitometric analysis of A. –RT, negative control.

0.75x NAM containing 0.1% bovine serum albumin (BSA) and 5 ng/ml recombinant human Activin A (SIGMA). The explants were cultured at stages 16–17 in the presence or absence of dexamethasone and harvested for RT-PCR experiments. For mesoderm explant assays, *paraxisMO* or *CtrMO* was injected into the marginal zone of both dorsal blastomeres of four-cell stage embryos. Mesoderm explants were dissected at stage 12 and cultured on agar in 1x MBR solution. The explants were photographed at stages 16–17 and harvested for RT-PCR experiments.

Scanning Electron Microscopy

The vitelline membrane was removed from injected tail-bud embryos, which were then fixed by incubation in 3% glutaraldehyde/4% formaldehyde/phosphate saline buffer (PBS), and the dorsal epithelium was peeled away to show the mesodermal tissue. The treated side of the embryos was previously determined by observation under a fluorescence stereomicroscope. The embryos were then gradually dehydrated in ethanol and critical point drying was performed in acetone and CO_2. Finally, the samples were coated with gold and observed using a JEOL 35CF Scanning Electron Microscope.

Nuclear Staining

Nuclei were stained with DAPI. Embryos were embedded in paraffin and sectioned (7 μm). Sections were then incubated in xylene, rehydrated by incubation in a graded series of ethanol concentrations, washed in PBS, and incubated with DAPI (1 μg/ml in PBS) at room temperature for 10 min. Finally, sections were thoroughly washed, mounted, and observed with an Olympus BX80 epifluorescence microscope.

Whole-Mount In Situ Hybridization and Immunohistochemical

Embryo fixation and whole-mount in situ hybridization with digoxigenin-UTP RNA probes were carried out as previously described by Harland (1991), with minor modifications as described by Mayor et al. (1996) and Monsoro-Burq (2007). The probes used were *MyoD* (Hopwood et al., 1989), *Myf-5* (Hopwood et al., 1991), *pax1* and *pax9* (Sanchez and Sanchez, 2013), and *Col2A* (clone XL241d0, kindly provided by Dr. Naoto Ueno, NIBB, Okazaki, Japan) was transcribed with SP6 RNA polymerase from pBluescript II templates linearized with *Xho*I. Detection of labeled probes was performed using alkaline-phosphatase conjugated anti-digoxigenin Fab fragments and with NBT/BCIP as substrate (Roche). Pigmented embryos were bleached with a solution containing 1% H_2O_2/PBS. To determine the effects of knocking down *paraxis* on myotome differentiation the embryos were unilaterally injected with *paraxisMO* or *CtrMO* and cultured until tail-bud stage. We used a standard immunostaining protocol described in the Cold Spring Harbor manual to visualize specific proteins (Khokha et al., 2002).

RNA Isolation and RT-PCR Expression Analysis

Total RNA was isolated from whole embryos using TRIREAGENT® reagent (MRC) according to manufacturer's instructions. cDNAs were synthesized by M-MLV Reverse Transcriptase (Promega) with oligo(dT^{15}) priming from 1 μg total RNA extracted from embryo and tissue explants. PCRs were performed with GoTaq polymerase (Promega) in semi-quantitative amplification conditions and *EF-1α* was used as an internal standard. The oligonucleotide primers and cycling conditions designed for this study were: *EF-1α*, 5′-CAG ATT GGT GCT GGA TAT GC-3′ and 5′-ACT GCC TTG ATG ACT CCT AG-3′, 25 cycles; *pax1*, 5′-CTA CCC TAC CAG CAA CCA ATA TG-3′ and 5′-CAA CTG TCC CAC TAA ATC ACC TC-3′, 29 cycles; *pax9*, 5′-AGT AGG AAC ACG TTT CAG TCG-3′ and 5′-TTG GAT CCT AGA GAT GAC AGC-3′, 30 cycles; *uncx*, 5′-TTA AGA CCC TGG AGG TGT GG-3′ and 5′-TGT TTT CGC CCC TGT AAT TC-3′, 30 cycles; *EP-cadherin*, 5′-AGG AAG GTG GAG AGG AG-3′ and 5′-GAG AGT CAT ATG GGG GAG CA-3′, 28 cycles; *E-cadherin*, 5′-CGA AGA TGT AAA CGA AGC C-3′ and 5′-GCC ATT TCC AGT GAC AAT C-3′, 30 cycles; *FoxC1*, 5′-CTG CAG CAA ATT CTG ACC AA-3′ and 5′-ACC TTA CGA GAT TGC CAT GC-3′, 27 cycles; *Integrin α5*, 5′-TGA TGC TGG TCA AGG G-3′ and 5′-ATG AAG CCG CCT GTC GTG TC-3′, 30 cycles; *Myf-5*, 5′-CGA TCT ACA GAC AAG TTT CTC TTC AAC CAA-3′

and 5′-GTA GGA GAC GGG GTG ATA GAG TCT GGA ATA-3′, 30 cycles, *MyoD*, 5′-AGC TCC AAC TGC TCC GAC GGC ATG AA-3′ and 5′-AGG AGA GAA TCC AGT TGA TGG AAA CA-3′, 28 cycles; *occludin*, 5′-CCG ACG AGT TGG AAG ATG AT-3′ and 5′-TGA TTT CCT TAA GCC GGT TG-3′, 30 cycles; *pax3*, 5′-AGG AGA CCG GAT CCA TCA GA-3′ and 5′-TGG AGC TTA CCG GGT TGT CT-3′, 28 cycles; *Xbra*, 5′-GCT GGA AGT ATG TGA ATG GAG-3′ and 5′-TTA AGT GCT GTA ATC TCT TCA-3′, 29 cycles. The PCR products were analyzed on 1.5% agarose gels. As a negative control, PCR was performed with RNA that had not been reverse-transcribed to check for DNA contamination. The relative intensity of PCR bands was semi-quantified using the public domain software ImageJ (http://rsb.info.nih.gov/ij/) with data obtained from two independent experiments.

Western Blot Analysis

Injected or control embryos were homogenized in lysis buffer containing 50 mM Tris–HCl pH 7.4, 0.1 M NaCl, 1% Nonidet P-40, 2 mM PMSF (Roche), and then sonicated (three times, 10 s each, midpower) on ice. Protein concentration was determined by Lowry's method (Lowry et al., 1951).The samples were boiled for 4 min in 2% sodium dodecyl sulfate (SDS), 2% 2-mercaptoethanol, 20 mM Tris–HCl, pH 7, and placed (20 μg of protein/lane) on 7.5% SDS–polyacrylamide gel. After electrophoresis, the proteins were transferred to a nitrocellulose membrane (Hybond-C super; Amersham, Buckinghamshire, UK). Nonspecific binding to the membrane was blocked for 1 hr at room temperature with 5% (w/v) BSA in Tris-buffered saline buffer (20 mmol/L Tris–HCl, 150 mmol/L NaCl, and 0.1% [v/v] Tween 20). The membranes were then incubated overnight at 4°C with rabbit anti-GFP polyclonal antibody (Molecular Probes, A-6455) or rabbit anti-fibronectin polyclonal antibody (Santa cruz, H300). After washing, the membranes were incubated with mouse anti-rabbit antibody with biotin conjugate (Sigma, B3275) and developed using a biotin-Streptavidin-AP *Systems* (Promega). Phophatase activity was detected by incubating blots in NBT/BCIP. γ-tubulin was used as loading control (SIGMA, T3320).

Acknowledgments

We thank Naoto Ueno for the EST XL013c24 and XL241d03 clones, J.B. Gurdon for providing *MyoD* and *Myf-5* plasmids for in situ hybridization and Cirio Maria for 102/12 antibody. We are grateful to LAMENOA (Laboratorio de Microscopía Electróica del Noroeste Argentino) for their Scanning Electron Microscopy observations. We also thank Dra. Marcela Bonano for her constructive criticism of the manuscript. This research was supported by Consejo Nacional de Investigaciones Científicas y Técnicas (CONICET) and CIUNT grants to S.S.S. and Agencia Nacional de Promoción Científica y Tecnológica (FONCYT), Argentina. R.S.S. is a recipient of a CONICET (Argentina) Fellowship. S.S.S. is a Career Investigator of CONICET (Argentina). We also wish to thank Ms. Virginia Mendez for proofreading the text.

References

Afonin B, Ho M, Gustin JK, Meloty-Kapella C, Domingo CR. 2006. Cell behaviors associated with somite segmentation and rotation in Xenopus laevis. Dev Dyn 235:3268–3279.

Barnes GL, Alexander PG, Hsu CW, Mariani BD, Tuan RS. 1997. Cloning and characterization of chicken Paraxis: a regulator of paraxial mesoderm development and somite formation. Dev Biol 189:95–111.

Brand-Saberi B, Wilting J, Ebensperger C, Christ B. 1996. The formation of somite compartments in the avian embryo. Int J Dev Biol 40:411–420.

Buckingham M, Vincent SD. 2009. Distinct and dynamic myogenic populations in the vertebrate embryo. Curr Opin Genet Dev 19: 444–453.

Burgess R, Cserjesi P, Ligon KL, Olson EN. 1995. Paraxis: a basic helix-loop-helix protein expressed in paraxial mesoderm and developing somites. Dev Biol 168:296–306.

Burgess R, Rawls A, Brown D, Bradley A, Olson EN. 1996. Requirement of the paraxis gene for somite formation and musculoskeletal patterning. Nature 384:570–573.

Carpio R, Honore SM, Araya C, Mayor R. 2004. Xenopus paraxis homologue shows novel domains of expression. Dev Dyn 231: 609–613.

Cha JY, Birsoy B, Kofron M, Mahoney E, Lang S, Wylie C, Heasman J. 2007. The role of FoxC1 in early Xenopus development. Dev Dyn 236:2731–2741.

Christ B, Ordahl CP. 1995. Early stages of chick somite development. Anat Embryol (Berl) 191:381–396.

Della Gaspera B, Armand AS, Lecolle S, Charbonnier F, Chanoine C. 2012. Mef2d acts upstream of muscle identity genes and couples lateral myogenesis to dermomyotome formation in Xenopus laevis. PloS One 7:e52359.

Franz T, Kothary R, Surani MA, Halata Z, Grim M. 1993. The Splotch mutation interferes with muscle development in the limbs. Anat Embryol (Berl) 187:153–160.

Giacomello E, Vallin J, Morali O, Coulter IS, Boulekbache H, Thiery JP, Broders F. 2002. Type I cadherins are required for differentiation and coordinated rotation in Xenopus laevis somitogenesis. Int J Dev Biol 46:785–792.

Goulding M, Sterrer S, Fleming J, Balling R, Nadeau J, Moore KJ, Brown SD, Steel KP, Gruss P. 1993. Analysis of the Pax-3 gene in the mouse mutant splotch. Genomics 17:355–363.

Hamilton L. 1969. The formation of somites in Xenopus. J Embryol Exp Morphol 22:253–264.

Harland RM. 1991. In situ hybridization: an improved whole-mount method for Xenopus embryos. Methods Cell Biol 36:685–695.

Henry CA, Hall LA, Burr Hille M, Solnica-Krezel L, Cooper MS. 2000. Somites in zebrafish doubly mutant for knypek and trilobite form without internal mesenchymal cells or compaction. Curr Biol 10:1063–1066.

Hidalgo M, Sirour C, Bello V, Moreau N, Beaudry M, Darribere T. 2009. In vivo analyzes of dystroglycan function during somitogenesis in Xenopus laevis. Dev Dyn 238:1332–1345.

Hinits Y, Osborn DP, Hughes SM. 2009. Differential requirements for myogenic regulatory factors distinguish medial and lateral somitic, cranial and fin muscle fibre populations. Development 136:403–414.

Hopwood ND, Pluck A, Gurdon JB. 1989. MyoD expression in the forming somites is an early response to mesoderm induction in Xenopus embryos. EMBO J 8:3409–3417.

Hopwood ND, Pluck A, Gurdon JB. 1991. Xenopus Myf-5 marks early muscle cells and can activate muscle genes ectopically in early embryos. Development 111:551–560.

Johnson J, Rhee J, Parsons SM, Brown D, Olson EN, Rawls A. 2001. The anterior/posterior polarity of somites is disrupted in paraxis-deficient mice. Dev Biol 229:176–187.

Keller R. 2000. The origin and morphogenesis of amphibian somites. Curr Top Dev Biol 47:183–246.

Keller R, Danilchik M. 1988. Regional expression, pattern and timing of convergence and extension during gastrulation of Xenopus laevis. Development 103:193–209.

Keynes RJ, Stern CD. 1988. Mechanisms of vertebrate segmentation. Development 103:413–429.

Khokha MK, Chung C, Bustamante EL, Gaw LW, Trott KA, Yeh J, Lim N, Lin JC, Taverner N, Amaya E, Papalopulu N, Smith JC, Zorn AM, Harland RM, Grammer TC. 2002. Techniques and probes for the study of Xenopus tropicalis development. Dev Dyn 225:499–510.

Kragtorp KA, Miller JR. 2007. Integrin alpha5 is required for somite rotation and boundary formation in Xenopus. Dev Dyn 236:2713–2720.

Kulesa PM, Fraser SE. 2002. Cell dynamics during somite boundary formation revealed by time-lapse analysis. Science 298:991–995.
Leitges M, Neidhardt L, Haenig B, Herrmann BG, Kispert A. 2000. The paired homeobox gene Uncx4.1 specifies pedicles, transverse processes and proximal ribs of the vertebral column. Development 127:2259–2267.
Lowry OH, Rosebrough NJ, Farr AL, Randall RJ. 1951. Protein measurement with the Folin phenol reagent. J Biol Chem 193: 265–275.
Ludolph DC, Neff AW, Mescher AL, Malacinski GM, Parker MA, Smith RC. 1994. Overexpression of XMyoD or XMyf5 in Xenopus embryos induces the formation of enlarged myotomes through recruitment of cells of nonsomitic lineage. Dev Biol 166:18–33.
Mancilla A, Mayor R. 1996. Neural crest formation in Xenopus laevis: mechanisms of Xslug induction. Dev Biol 177:580–589.
Mansouri A, Voss AK, Thomas T, Yokota Y, Gruss P. 2000. Uncx4.1 is required for the formation of the pedicles and proximal ribs and acts upstream of Pax9. Development 127:2251–2258.
Maves L, Waskiewicz AJ, Paul B, Cao Y, Tyler A, Moens CB, Tapscott SJ. 2007. Pbx homeodomain proteins direct Myod activity to promote fast-muscle differentiation. Development 134:3371–3382.
Monsoro-Burq AH. 2007. A rapid protocol for whole-mount in situ hybridization on Xenopus embryos. CSH Protoc 2007: pdb.prot4809.
Nieuwkoop PD, Faber J. 1967. Normal table of Xenopus laevis (Daudin). Amsterdam: North-Holland Publishing Co.
Ostrovsky D, Sanger JW, Lash JW. 1988. Somitogenesis in the mouse embryo. Cell Differ 23:17–25.
Peters H, Wilm B, Sakai N, Imai K, Maas R, Balling R. 1999. Pax1 and Pax9 synergistically regulate vertebral column development. Development 126:5399–5408.
Pourquie O, Tam PP. 2001. A nomenclature for prospective somites and phases of cyclic gene expression in the presomitic mesoderm. Dev Cell 1:619–620.
Quertermous EE, Hidai H, Blanar MA, Quertermous T. 1994. Cloning and characterization of a basic helix-loop-helix protein expressed in early mesoderm and the developing somites. Proc Natl Acad Sci U S A 91:7066–7070.
Rodrigo I, Hill RE, Balling R, Munsterberg A, Imai K. 2003. Pax1 and Pax9 activate Bapx1 to induce chondrogenic differentiation in the sclerotome. Development 130:473–482.
Rowton M, Ramos P, Anderson DM, Rhee JM, Cunliffe HE, Rawls A. 2013. Regulation of mesenchymal-to-epithelial transition by PARAXIS during somitogenesis. Dev Dyn 242:1332–1344.
Sanchez RS, Sanchez SS. 2013. Characterization of pax1, pax9, and uncx sclerotomal genes during Xenopus laevis embryogenesis. Dev Dyn 242:572–579.
Shanmugalingam S, Wilson SW. 1998. Isolation, expression and regulation of a zebrafish paraxis homologue. Mech Dev 78:85–89.
Tajbakhsh S, Rocancourt D, Cossu G, Buckingham M. 1997. Redefining the genetic hierarchies controlling skeletal myogenesis: Pax-3 and Myf-5 act upstream of MyoD. Cell 89:127–138.
Takahashi Y, Takagi A, Hiraoka S, Koseki H, Kanno J, Rawls A, Saga Y. 2007. Transcription factors Mesp2 and Paraxis have critical roles in axial musculoskeletal formation. Dev Dyn 236:1484–1494.
Tremblay P, Dietrich S, Mericskay M, Schubert FR, Li Z, Paulin D. 1998. A crucial role for Pax3 in the development of the hypaxial musculature and the long-range migration of muscle precursors. Dev Biol 203:49–61.
Tseng HT, Jamrich M. 2004. Identification and developmental expression of Xenopus paraxis. Int J Dev Biol 48:1155–1158.
Wallin J, Wilting J, Koseki H, Fritsch R, Christ B, Balling R. 1994. The role of Pax-1 in axial skeleton development. Development 120:1109–1121.
Wilson-Rawls J, Hurt CR, Parsons SM, Rawls A. 1999. Differential regulation of epaxial and hypaxial muscle development by paraxis. Development 126:5217–5229.
Wilson-Rawls J, Rhee JM, Rawls A. 2004. Paraxis is a basic helix-loop-helix protein that positively regulates transcription through binding to specific E-box elements. J Biol Chem 279:37685–37692.
Wilson PA, Oster G, Keller R. 1989. Cell rearrangement and segmentation in Xenopus: direct observation of cultured explants. Development 105:155–166.
Youn BW, Malacinski GM. 1981a. Comparative analysis of amphibian somite morphogenesis: cell rearrangement patterns during rosette formation and myoblast fusion. J Embryol Exp Morphol 66:1–26.
Youn BW, Malacinski GM. 1981b. Somitogenesis in the amphibian Xenopus laevis: scanning electron microscopic analysis of intrasomitic cellular arrangements during somite rotation. J Embryol Exp Morphol 64:23–43.

Developmental Dynamics